Front. Optoelectron. China 2010, 3(3): 253–259
DOI 10.1007/s12200-010-0107-8

RESEARCH ARTICLE

Experimental investigation into conversion efficiency of cascading four-wave mixing

Liang ZHAO, Junqiang SUN (✉)

Wuhan National Laboratory for optoelectronics, College of Optoelectronic Science and Engineering, Huazhong University of Science and Technology, Wuhan 430074, China

© Higher Education Press and Springer-Verlag Berlin Heidelberg 2010

Abstract We have proposed and experimentally demonstrated a scheme for cascading four-wave mixing (CFWM) by exploiting nonlinearity in highly nonlinear fiber (HNLF). Through utilizing optical spectrum analyzer (OSA), the second-order sideband products are observed in our experiment by only launching two waves into HNLF, and the conversion efficiency from the injected wave to each sideband is discussed in detail. It is found that only the conversion efficiency of the satellite wave will be increased with the power of the tunable injected wave when the power and the wavelength of the other one are fixed. Furthermore, the conversion efficiency of all the sidebands will be decreased with the absolute value of detune of injected wavelengths increasing. Also, the authors have demonstrated that the power of the satellite wave will be influenced most among all the sidebands if tuning the injected wave power. The proposed scheme can find potential applications in parametric amplification, frequency conversion, and optical quantum-information processing.

Keywords highly nonlinear fiber, cascading four-wave mixing, optical spectrum analyzer, conversion efficiency

1 Introduction

Fiber four-wave mixing (FWM) is a phenomenon attracting increased attention in optical fiber communications. Generally speaking, FWM contains two types: one is the well-known degenerate FWM with only one pump, and the other is the non-degenerate FWM with two pumps injected in the system. Furthermore, Thompson et al. [1] have proposed and derived the coupled-mode equations for multiple FWM (MFWM) processes, which can be interpreted by the following mechanism: if the powers of the injected waves are intense enough, the powers of the sideband products caused by MFWM are also very large, which will beat with the injected wave, and the second-order product is generated. In 2005, Liu et al. have proposed a model for MFWM processes with only two pumps involved, where the self-stability function of such FWM processes is revealed [2]. In 2008, Liu has also proposed a model concerning more than two pumps and has experimentally confirmed the stabilization of waves in MFWM processes [3]. The MFWM has wide applications in parametric amplification [4], frequency conversion [5], and optical quantum-information processing, especially in the region of 2R and 3R regeneration [6].

Although MFWM processes have been extensively investigated in the past years, cascading four-wave mixing (CFWM) processes have seldom been reported for the author's best knowledge. The main difference between MFWM and CFWM is that we only consider the first sideband products of FWM in the former, while the second-order or even higher-order products will be taken into account of in the latter. In our proposed model, the CFWM configuration is proposed, and the conversion efficiency of all the products containing the first-order products and higher-order products has been experimentally investigated with the results that only the satellite wave's conversion efficiency will be increased with the injected wave power. Moreover, the detune of injected wavelengths that influences the conversion efficiency is also considered.

2 Experimental setup and principal

Figure 1 schematically illustrates the diagram of frequency components generated owing to CFWM principal when

Received May 14, 2010; accepted May 27, 2010

E-mail: jqsun@mail.hust.edu.cn

two waves at angular frequencies ω_1 and ω_2 seeded in the highly nonlinear fiber (HNLF), respectively. Remarkably, if the power of the injected wave is high enough, the second-order sidebands may be generated, i.e., the wave with angular frequency ω_5 or ω_6, and the evolution of each wave is strictly governed by coupled wave equations [2,3,7]. Note that, the angular frequency relations for both the injected waves and sidebands can be given by

$$\begin{aligned} 2\omega_3 &= \omega_1 + \omega_5, \\ 2\omega_1 &= \omega_2 + \omega_3, \\ 2\omega_2 &= \omega_1 + \omega_4, \\ 2\omega_4 &= \omega_2 + \omega_6; \end{aligned} \tag{1}$$

$$\begin{aligned} \omega_1 + \omega_3 &= \omega_2 + \omega_5, \\ \omega_1 + \omega_2 &= \omega_3 + \omega_4, \\ \omega_2 + \omega_4 &= \omega_1 + \omega_6, \end{aligned} \tag{2}$$

where Eqs. (1) and (2) describe the degenerate and non-degenerate processes in the CFWM, respectively. The final output optical spectrum is the synthetic result of the single process competing with each other [7]. In the following experimental discussion, the conversion efficiency is our main concern, and the definition of conversion efficiency can be given by

$$\eta_{1\to j} = 10\log\frac{P_j}{P_1}, \quad j = 5,3,4,6; \tag{3}$$

$$\eta_{2\to j} = 10\log\frac{P_j}{P_2}, \quad j = 5,3,4,6, \tag{4}$$

where $\eta_{1\to j}$ or $\eta_{2\to j}$ denotes the conversion efficiency from wave 1 to sidebands or from wave 2 to sidebands, respectively. Remarkably, when testing the conversion efficiency, we will fix an injected wave and tune the wavelength or the power of the other injected wave, i.e., if calculating $\eta_{1\to j}$, the wavelength and injected power of wave 2 are fixed, and simultaneously, we record the sideband power P_j when we tune the wavelength of wave 1, as shown in Fig. 1.

Figure 2 schematically illustrates the experimental setup for CFWM in the HNLF. Two waves emitted from the tunable lasers (TLs) are both launched into the 3-dB coupler, and they are modulated with a phase modulator (PM) using a 2.5-GHz pseudorandom binary sequence (PRBS) with pattern length $2^{15}-1$ in order to increase bandwidth of wave 1, leading to suppression of stimulated Brillouin scatter (SBS) [8]. The isolator (ISO) is used to make sure the unidirection propagation of the waves. The modulated waves are then amplified by high power erbium-doped fiber amplifier (HP-EDFA) to enhance the FWM efficiency. After passing through the HNLF, the generated sidebands are monitored by

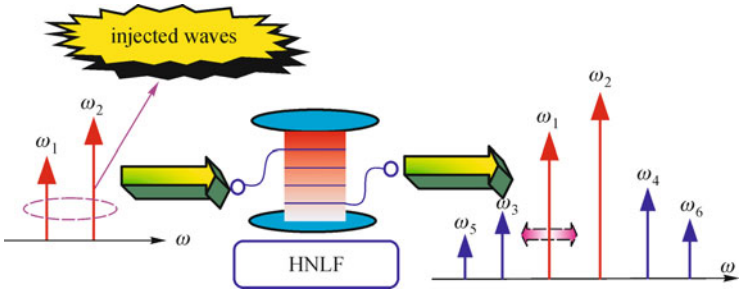


Fig. 1 Schematic diagram of frequency components generated due to CFWM for two waves at frequencies ω_1, and ω_2 seeded in HNLF, respectively

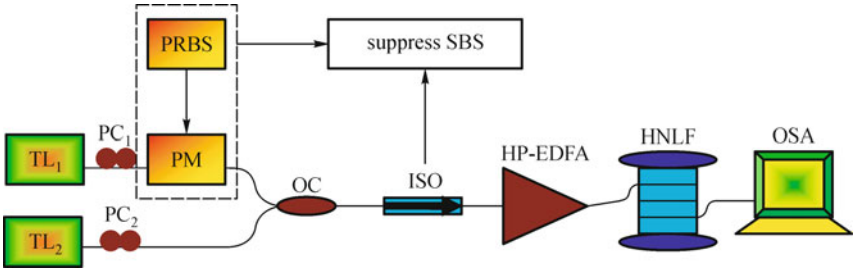


Fig. 2 Experimental setup for CFWM in HNLF (TLs: tunable lasers; OC: 3-dB optical coupler; PC: polarization controller; OSA: optical spectrum analyzer; HP-EDFA: high power erbium-doped fiber amplifier; HNLF: highly nonlinear fiber; ISO: isolator; PRBS: pseudorandom binary sequence; PM: phase modulator; SBS: stimulated Brillouin scatter)

the optical spectrum analyzer (OSA). Additionally, HNLF is structured with the length 135 m and the zero-wavelength 1552 nm, and the nonlinear coefficient is 20 $(W \cdot km)^{-1}$.

3 Experimental results and discussion

Figure 3 demonstrates each sideband power together with corresponding conversion efficiency as a function of the power of wave 1 when the wavelengths tuned at 1551.913 and 1552.549 nm, respectively. It can be clearly found that each sideband power will be increased with the power of wave 1 since its power is increased with the product of the injected wave powers [2,3,7,9,10]. However, the conversion efficiency from wave 1 to each sideband takes on different characteristics. In detail, the conversion efficiency $\eta_{1\to 3}$ is increased with the power of wave 1 (see the red line in Fig. 3(b)), while $\eta_{1\to j}$ $(j=4,5,6)$ is decreased with the power of wave 1. In order to unveil the intrinsic physical mechanism, it is necessary to introduce the notion of the satellite wave, which is defined as the sideband with the smallest detune compared to the injected wave, i.e., see Fig. 4, wave 3 is the satellite wave compared to wave 1, whereas wave 4 is the satellite wave compared to wave 2. In other words, only the conversion efficiency of the satellite wave will be increased with the power of wave 1. This can also be explained from the coupled wave Eqs. (2) and (3) that $\partial P_3/\partial z \propto P_1$ and $\partial P_j/\partial z \propto \sqrt{P_1}$ $(j=4,5,6)$, which implies that the increasing rate of the satellite wave is larger than that of other sidebands, and P_j represents the power of each sideband.

Figure 4 further illustrates the output optical spectrum with the parameters set as λ_1= 1551.913 nm, λ_2= 1552.549 nm and P_1= 4.725, 0.85 and −5.472 dBm, respectively. In an intuitive approach, it can be clearly seen that when wave 1 ranges from −5.472 to 4.725 dBm, the power of the satellite wave will be influenced most with ΔP_1 = 10.197 dB. Again, in this case, we confirm that, at the same condition, the varying rate of the satellite is much faster than that of other sidebands, even exceeding with that of wave 1.

In order to further confirm the property of the satellite wave, similar experiment is carried out with injected wavelengths tuned at 1550.9 and 1551.3 nm, and Fig. 5 also shows each sideband power together with the corresponding conversion efficiency vs the power of wave 2. Differently, in this case, the power of wave 2 (larger injected wavelength) ranges from −20 to 7 dBm, with the fixed power and wavelength of wave 1 tuned at 8.03 dBm and 1551.3 nm. From the red dashed line in

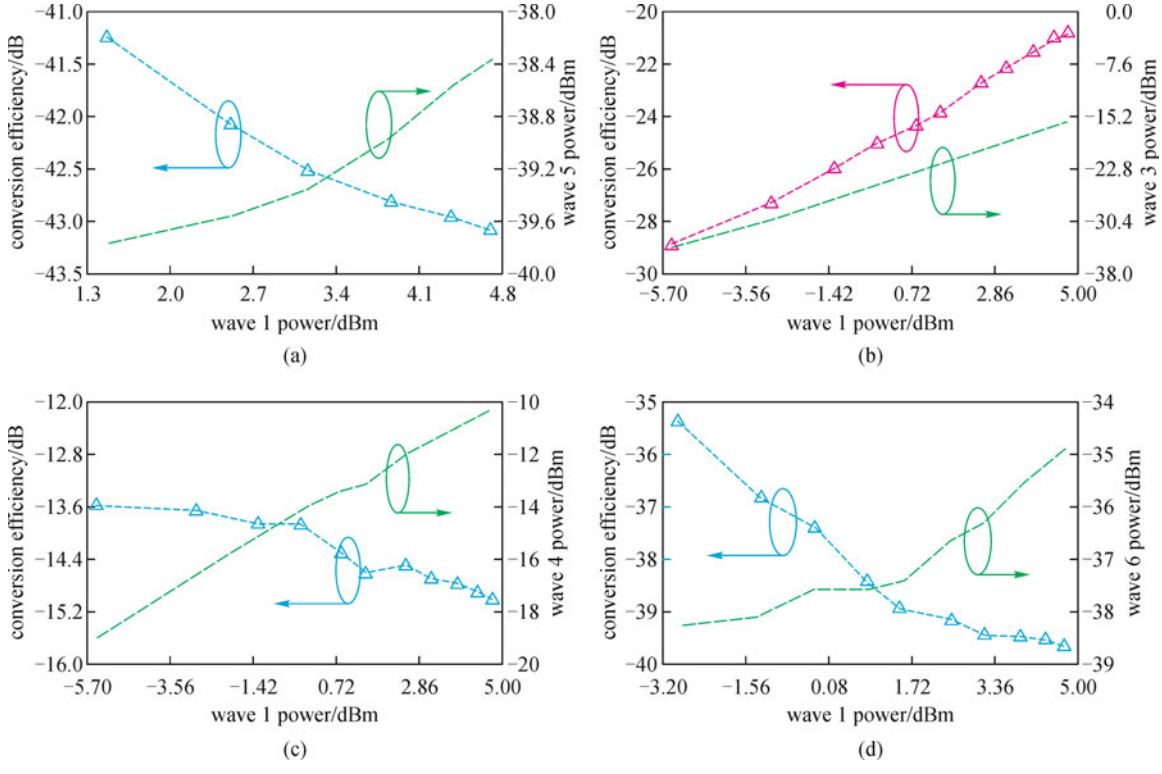


Fig. 3 Each sideband power together with corresponding conversion efficiency vs power of wave 1 when injected wavelengths are tuned at 1551.913 and 1552.549 nm, respectively. (a) Wave 5; (b) wave 3; (c) wave 4; (d) wave 6

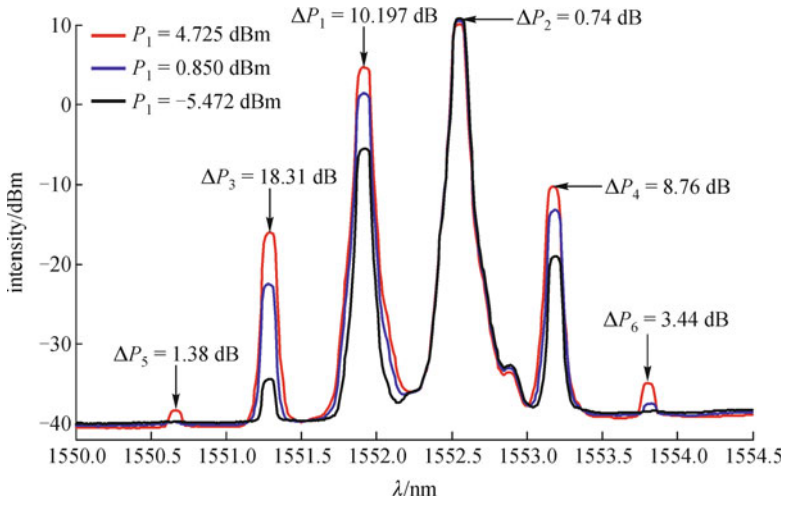


Fig. 4 Output optical spectrum when injected wavelengths tuned at 1551.913 and 1552.549 nm, respectively, with power of wave 1 adjusting at 4.725, 0.85 and −5.472 dBm (initial power of wave 2 is tuned at about 10.12 dBm)

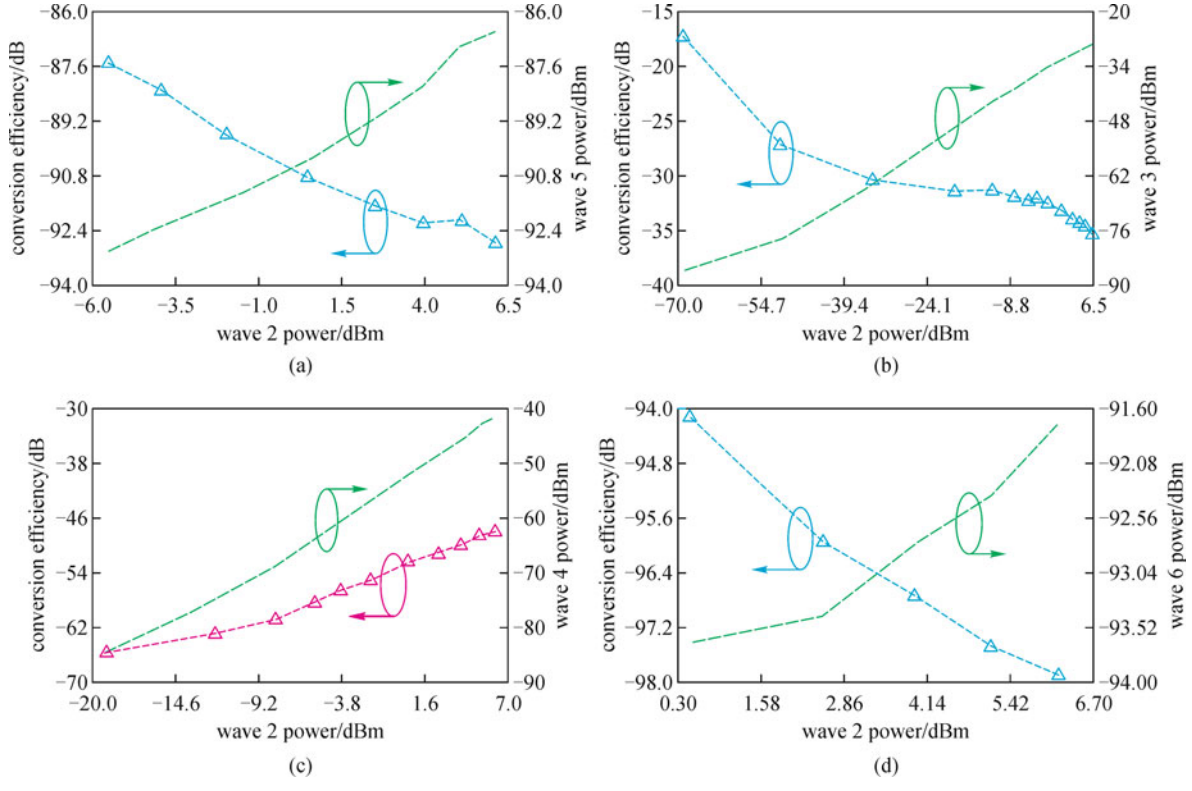


Fig. 5 Each sideband power together with corresponding conversion efficiency vs power of wave 2 when injected wavelengths are tuned at 1550.9 and 1551.3 nm, respectively. (a) Wave 5; (b) wave 3; (c) wave 4; (d) wave 6

Fig. 5(c), it can be also found that only the satellite wave (wave 4) conversion efficiency is increased with the power of wave 2. Furthermore, all the sideband powers will be increased with the wave 2 power, which is consistent with the previous conclusion.

Also, as a supplement of Fig. 5, Fig. 6 illustrates the output optical spectrum when injected wavelengths tuned at 1550.9 and 1551.3 nm, respectively, with the power of wave 2 adjusting at 6.16, 2.53 and −5.52 dBm. From the plot, we find that when ΔP_2= 5.118 dB, ΔP_4= 9.54 dB is

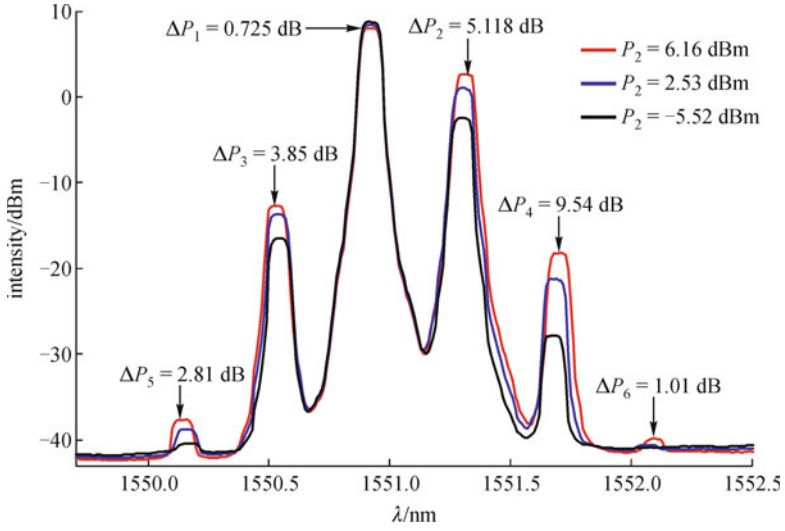


Fig. 6 Output optical spectrum when injected wavelengths tuned at 1550.9 and 1551.3 nm, respectively, with power of wave 2 adjusting at 6.16, 2.53 and –5.52 dBm (initial power of wave 1 is tuned at about 8.03 dBm)

the largest varying range among all the sidebands, which again proves that tuning the power of wave 2 will influence most to the power of the satellite wave.

A deep-rooted analysis on the detune of injected wavelengths influencing the conversion efficiency is also demonstrated, while Fig. 7 illustrates the conversion efficiency as a function of $\Delta\lambda$ with λ_2 = 1545.1 nm and P_2 = 8.5 dBm. Especially, Fig. 7(a) represents the conversion efficiency from wave 1 to sidebands when the wavelength of wave 1 is less than that of wave 2, from which it can be found that $\eta_{1\to3}$, $\eta_{1\to4}$ and $\eta_{1\to5}$ will be increased with the absolute value of $\Delta\lambda$ decreasing, but $\eta_{1\to6}$ will firstly be decreased and then increased with the absolute value of $\Delta\lambda$ decreasing, which can be ascribed to the following reasons. Firstly, a well-known regulation is that the smaller the detune of injected wavelengths is, the more energy will be transferred from the injected wave to the sidebands. Thus, $\eta_{1\to3}$, $\eta_{1\to4}$ and $\eta_{1\to5}$ will be increased if the absolute value of $\Delta\lambda$ decreases. Secondly, the power of wave 1 will be unavoidably increasing as λ_1 is approaching to λ_2 owing to the uneven amplified spontaneous emission (ASE) spectrum. As seen in Fig. 8, if the wavelength of wave 1 ranges from 1535 to 1545 nm, the ASE spectrum is tilting, which implies that the power of the injected wave will be amplified in different extents. Therefore, the power of wave 1 at the entry of HNLF will range from about −15 to 2 dBm, but the increasing rate of the power of wave 6 is less than that of wave 1, leading to subtle decreasing of the conversion efficiency. Additionally, if the absolute value of $\Delta\lambda$ is less than 0.33 nm, the energy flowing from wave 1 to wave 6 is sharply enhanced, and thus, the conversion efficiency will be increasing at last. Similar experimental results are shown in Fig. 7(b), which demonstrates $\eta_{2\to j}$ vs $\Delta\lambda$. Differently, the conversion efficiency of wave 6 will be first invariable and then increased with the absolute value of $\Delta\lambda$ decreasing owing to the power of wave 2 keeping in the level of about 8.5 dBm. At last, in Fig. 7(c), $\Delta\lambda$ is divided into three sections with region 1 (−1.667, 0), region 2 (−6.455, 0), and region 3 (−8.934, 0). Wave 5 and wave 6 can be observed if the wavelength of wave 2 is located at region 1, and wave 3 will be observed if the wavelength of wave 2 is located at region 2, whereas wave 4 can be observed if the wavelength of wave 2 is located at region 3. Otherwise, the power of generated sidebands is so low that the sidebands will be submerged in the ASE spectrum.

4 Conclusions

We have proposed and demonstrated a scheme for CFWM by exploiting nonlinearity in HNLF. The second-order sideband products are observed in our experiment by only launching two waves into our system, and the conversion efficiency from the injected wave to each sideband is investigated in detail, with the conclusion being drawn as: 1) the powers of all the sidebands are increased with the power of the tunable injected wave; 2) only the conversion efficiency of the satellite wave will be increased with the power of the injected wave; 3) the conversion efficiency of all the sidebands will be decreased with the absolute value of detune of injected wavelengths increasing. The proposed scheme can find potential applications in parametric amplification, frequency conversion, and optical quantum-information processing.

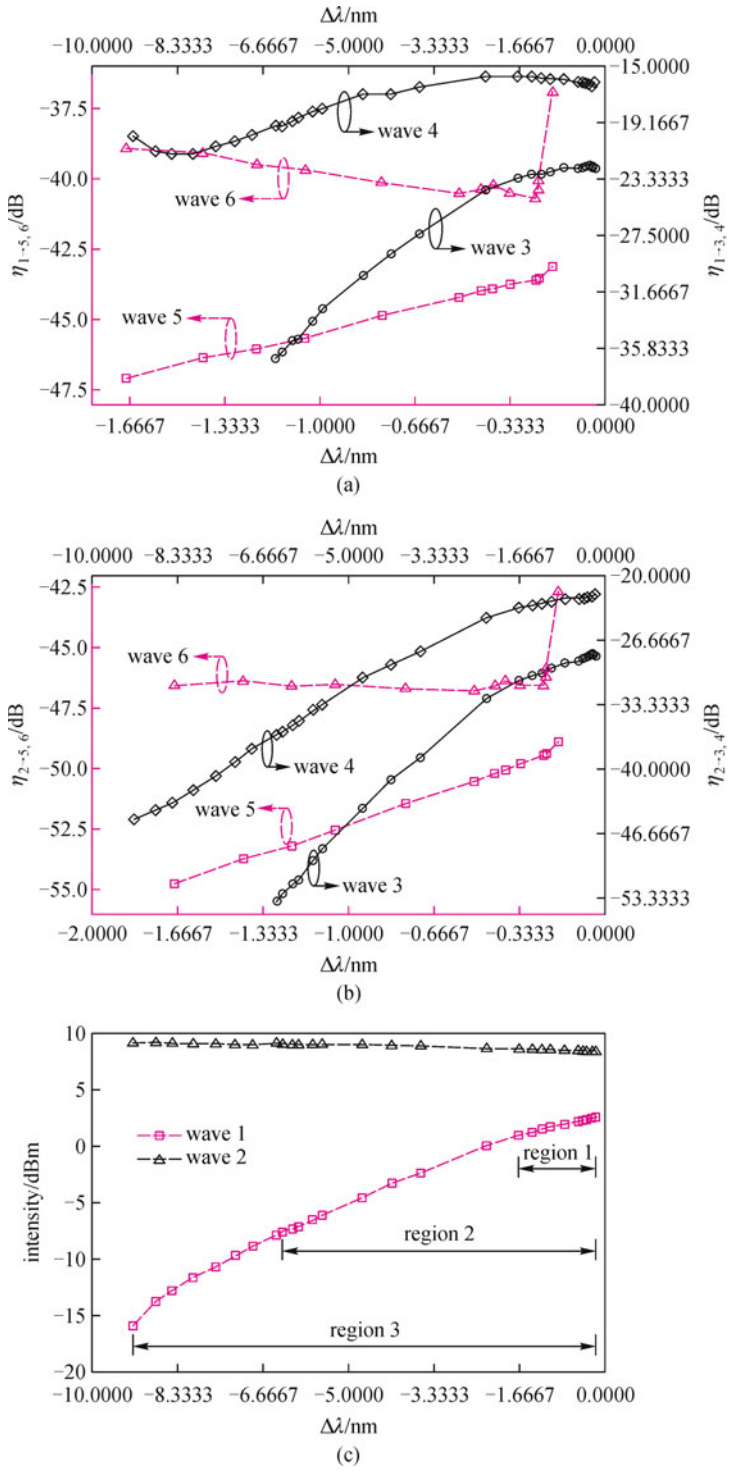


Fig. 7 Function of detune of injected wavelengths $\Delta\lambda$. (a) $\eta_{1\rightarrow j}$; (b) $\eta_{2\rightarrow j}$; (c) powers of injected waves vs $\Delta\lambda$ (other parameters are set as $\lambda_2 = 1545.1$ nm while $\lambda_1 < \lambda_2$)

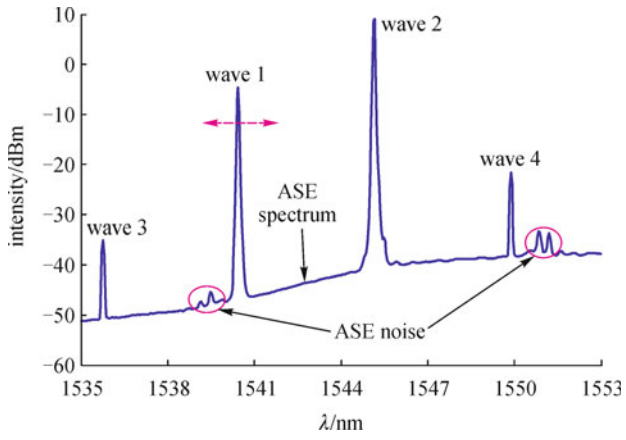


Fig. 8 Optical spectrum together with ASE spectrum when wave 2 fixed with power 8.5 dBm and wavelength 1545.1 nm

References

1. Thompson J R, Roy R. Nonlinear dynamics of multiple four-wave mixing processes in a single-mode fiber. Physical Review A, 1991, 43(9): 4987–4996
2. Liu X M, Zhou X Q, Lu C. Multiple four-wave mixing self-stability in optical fibers. Physical Review A, 2005, 72(1): 013811
3. Liu X M. Theory and experiments for multiple four-wave-mixing processes with multifrequency pumps in optical fibers. Physical Review A, 2008, 77(4): 043818
4. Hugonnot E, Somekh M, Villate D, Salin F, Freysz E. Optical parametric chirped pulse amplification and spectral shaping of a continuum generated in a photonic band gap fiber. Optics Express, 2004, 12(11): 2397–2403
5. Sun J Q, Li H, Cheng Y, Li J. Tunable wavelength conversion of picosecond pulses based on cascaded sum- and difference-frequency generation in quasi-phase-matched $LiNbO_3$ waveguides. Optics Communications, 2008, 281(23): 5874–5883
6. Rochette M, Blows J L, Eggleton B J. 3R optical regeneration: an all-optical solution with BER improvement. Optics Express, 2006, 14(14): 6414–6427
7. Zhao L, Sun J Q, Suppression of degenerate four-wave mixing in nondegenerate optical parametric amplifiers. Optical Engineering, 2008, 47(8): 085001
8. Hansryd J, Andrekson P A, Westlund M, Li J, Hedekvist P O. Fiber-based optical parametric amplifiers and their applications. IEEE Journal of Selected Topics in Quantum Electronics, 2002, 8(3): 506–520
9. Zhao L, Sun J Q. Investigation of tunable trap filter utilizing intense signal four-wave mixing model in highly non-linear fiber. Optics Communications, 2009, 282(14): 2975–2982
10. Cao H, Sun J Q, Huang D X. Unique dispersion effects on transmitting and amplifying of picosecond pulses in fiber optical parametric amplifiers. Proceedings of SPIE, 2005, 6019: 662–670